Force Transmissibility Performance of Parallel Manipulators

Wen-Tung Chang and Chen-Chou Lin*
Department of Mechanical and Marine Engineering
National Taiwan Ocean University
Keelung, Taiwan, 20224, ROC
e-mail: wtchang@webmail.pme.nthu.edu.tw, cclin@euler.me.ntou.edu.tw

Jyh-Jone Lee
Department of Mechanical Engineering
National Taiwan University
Taipei, Taiwan, ROC
e-mail: jjlee@ntu.edu.tw

Received 18 March 2003; accepted 8 September 2003

In this paper, a new force transmission index called the mean force transmission index ($MFTI$) is proposed, and the force transmissibility analysis procedure is established for parallel manipulators. The $MFTI$ is an extended definition of the force transmission index (FTI) introduced by the authors previously. It is shown that the FTI is a function of the input velocity ratio (IVR) for a multi-DOF mechanism of the same configuration. To represent the force transmissibility by a definite value, the $MFTI$ is defined as the mean value of the normalized FTIs function over the whole range of the IVR. The force transmissibility analysis of two planar parallel manipulators is illustrated using the $MFTI$ method. The result is compared with that of the Jacobian matrix method and the joint force index (JFI) method. It shows that, especially for symmetric parallel manipulators, an approximate inverse-proportionality relationship exists between the JFI and $MFTI$, and between the maximum input torque/force and $MFTI$. It is concluded that the $MFTI$ can be used as a quantitative measure of the force transmissibility performance for parallel manipulators. In the end, a design optimization problem is studied by taking the global force transmission index as the objective function.

*To whom all correspondence should be addressed.

Journal of Robotic Systems 20(11), 659–670 (2003) © 2003 Wiley Periodicals, Inc.
Published online in Wiley InterScience (www.interscience.wiley.com). • DOI: 10.1002/rob.10115

1. INTRODUCTION

Parallel manipulators have received extensive attention in the robotics society for the past two decades. Parallel manipulators are one type of multiple degree-of-freedom (DOF) closed-loop mechanisms with a moving platform supported by a number of in-parallel limbs. In general, they are characterized by a higher structural rigidity and larger load-carrying capacity as compared with the conventional serial-type manipulators. The applications of such manipulators are, for example, earthquake simulator, aircraft simulator, machining center, force-torque sensor, pointing device, etc.

Prior research about parallel manipulators focused primarily in the areas of the mechanism design, kinematic analysis, and performance analysis. For the performance analysis, existing studies usually deal with the investigations of the singularity,[1–9] manipulability,[10–12] workspace,[13–21] conditioning index,[22–24] and stiffness property.[23–27] The singularity of a mechanism which causes the instantaneous change of DOF is determined by the Jacobian matrix. Gosselin et al.[1] first studied the singularities of closed-loop mechanisms and suggested the separation of the Jacobian matrix into two submatrices: one associated with the forward kinematics and the other with the inverse kinematics. Zlatanov et al.[2] later redefined the classification of singularity. St-Onge et al.[6] studied the singularity of the general six-DOF platform based on analytical expressions of the determinant of the Jacobian matrix. They showed that, for a given orientation of the platform, the singularity locus in the Cartesian space is represented by a polynomial of degree three. Choudhury et al.[7] studied the kinematic and force singularities of parallel manipulators and closed-loop mechanisms. Park et al.[10] presented a differential geometric formulation of manipulability for general closed-loop mechanisms. Gosselin et al.[22] proposed a global performance criterion based on the condition number of the Jacobian matrix for the optimization of parallel robotic manipulators. Tsai et al.[24] optimized the global conditioning index to obtain the well-conditioned workspace and constructed the stiffness and inertia properties by the Jacobian matrix. In addition to the above performance criteria, the force transmission performance of parallel manipulators is considered important due to their payload capacity feature. Parallel manipulators with poor force transmission performance can not transmit power or force to counterbalance the external load efficiently. Denavit et al.[28] and Wu et al.[29] used the determinant of the Jacobian matrix as a transmission index. Tsai et al.[30] developed the generalized transmission wrench screw to measure the transmission performance of mechanisms. They pointed out that the transmission performance should take into account both the transmissibility and the manipulability of the mechanism. Takeda et al.[31] introduced a motion transmission index for parallel manipulators based on the definition of the minimum value of the cosine of the pressure angle. Holte et al.[32] pointed out that the external loads would affect the force transmission performance of a mechanism. They proposed the joint force index (JFI) as the ratio of the maximal joint force to the external load. Lin and Chang[33] pointed out that the Jacobian-based performance indices are configuration dependent only, meaning that they will not reflect the effects of different output links and the forms of the loading. They proposed the force transmission index (FTI) for general single-DOF linkage mechanisms and established a systematic analysis procedure. The FTI incorporates the concepts of power flow path, the effective force ratio of the output link and force gain per unit cost (input torque/force) of the input link. The analysis results showed that the FTI can describe the force transmissibility of the linkage mechanisms more accurately than other methods do. The feasibility of the FTI applied to other categories of linkages was also investigated by Lin et al.[34] and Chang.[35]

This paper aims to evaluate the force transmissibility of the parallel manipulators by introducing a systematic analysis procedure. The FTI introduced previously[33,34] is applicable to the single-DOF linkage mechanisms only. In this paper, we shall extend the FTI method by considering the effects of the input velocity ratios, and constitute a new index called the mean force transmission index ($MFTI$) for multi-DOF mechanisms. The force transmissibility performance analysis of two planar parallel manipulators is illustrated using the $MFTI$ method.

2. FORCE TRANSMISSION INDEX

We shall briefly review the definition of the FTI for single-DOF mechanisms first. Then the definition of the index will be extended to the multi-DOF mechanisms thereafter. In this paper, we shall follow the assumption that the gravitational forces, inertia forces, and frictional forces will not be considered.

In ref. 33, an input-related joint was defined as the joint at the output link where there is a path (a sequence of links and joints connected in series) connected to the input link. The *effective force ratio (EFR)* of an output link i was then defined as the total power

transmitted to the output link via the input-related joints versus the potential maximum power $p_{\max}$. That is,

$$R_i \equiv \frac{\Sigma_j p_{ji}}{p_{\max}} \tag{1a}$$

$$= \frac{\Sigma_j [f_j v_j \cos(\alpha_j) + \tau_j \omega \cos(\beta_j)]}{\Sigma_j (f_j v_j + \tau_j \omega)}, \tag{1b}$$

where f_j and v_j denote respectively the magnitude of the joint force and the absolute velocity of the input-related joint J_{ji}. α_j denotes the angle subtended between $\mathbf{f}_j$ and $\mathbf{v}_j$; τ_j and ω denote respectively the magnitude of the joint reaction moment of the input-related joint and the angular velocity of the output link. β_j denotes the angle subtended between τ_j and ω.

The EFR (R_i), ranging between –1 and +1, can be used as the measure of the proportion of the total effective force in the output link i, which will characterize the performance of the output link alone. To measure the force transmissibility of the whole mechanism, the capability of the input link for resisting the loading should be considered. Thus we defined the force transmissibility of a mechanism as the effective force gain (in the output link) versus the "cost" (input force/torque) paid by the input link with a fixed loading exerted on the output link. In ref. 33, the *force transmission index* was defined as *the effective force ratio per unit input torque/force, with a unit torque/force exerted on the output link i*. That is,

$$\tau \equiv \begin{cases} \left|\dfrac{R_i T'_{\text{out}}}{T'_{\text{in}}}\right| = \left|R_i \dfrac{T_{\text{out}}}{T_{\text{in}}}\right| = |R_i(MA)| \\ \quad \text{for pure moment loading and input} \\ \left|\dfrac{R_i F'_{\text{out}}}{F'_{\text{in}}}\right| = \left|R_i \dfrac{F_{\text{out}}}{F_{\text{in}}}\right| = |R_i(MA)| \\ \quad \text{for pure force loading and input} \end{cases}, \tag{2}$$

where R_i denotes the EFR of the output link i. MA denotes the mechanical advantage. T'_{in} (F'_{in}) is the magnitude of input torque (force) when a unit torque (force) ($T'_{\text{out}} = F'_{\text{out}} = 1$) is applied to the output link. T_{in}(F_{in}) is the magnitude of input torque (force) when an arbitrary amount of torque T_{out} (force F_{out}) is applied to the output. Note that we place the term T'_{out}(F'_{out}) in the numerator of the first term in (2) to make the index (τ) dimensionless.

The FTI is a dimensionless quantity which ranges between zero and positive infinity. The index can be used to describe the quality of the force transmissibility of the mechanism. For single-loop mechanisms, when the FTI vanishes, it indicates that the mechanism cannot transmit any effective force to the output link due to the divergence of the input torque/force.

The above FTI is physically meaningful; however, for the index to be more useful in representing the force transmission performance of a mechanism, the index should be bounded. Hence we devised a transformation which maps the FTI to a bounded range and preserves the original functionality. In ref. 34, an index called the *normalized force transmission index* ($NFTI, \tau_n$) was defined by the transformation as follows:

$$\tau_n = 1 - e^{-\lambda \tau} = 1 - \exp(-\lambda |R_i||MA|), \tag{3}$$

where λ ($0 < \lambda \leqslant 1$) is the weighting factor of the FTI (τ). Note that one should assign the same value of the weighting factor when comparing the performance between different mechanisms. In this paper, the value of λ is set to be one.

From (3) we may observe that τ_n will vanish as τ equals to zero, while τ_n will tend to one as τ diverges. Hence the normalized performance index is a bounded value, ranging between zero and one. The transformation function in (3) is a monotonic increasing function of τ, hence the mapping will preserve the original functionality of the FTI. In what follows, we shall use the bounded index, $NFTI$, to represent the force transmissibility for an individual limb of multi-DOF parallel manipulators.

3. FORCE TRANSMISSION INDEX FOR MULTI-DOF MECHANISMS

In this section, we shall extend the definitions of the previously introduced FTI to the category of multi-DOF mechanisms, specifically parallel manipulators. There are a variety of structural arrangements for parallel manipulators. One category is the so-called symmetric parallel manipulator, whose number of limbs is equal to the number of the DOF, and the type and the number of joints in all the limbs are arranged in an identical pattern (although their physical lengths can be different). Compared with asymmetric parallel manipulators, the design of the symmetric topologic structure is more frequently adopted. We shall further assume that there is only one actuator in

each limb. Hence there is only one input-related path in a limb, and each input-related path does not overlap with others.

3.1. Input Velocity Ratio

For single-DOF mechanisms, the EFR is independent of the magnitude of the input velocity since the proportional factor in the numerator and the denominator of (1) can be cancelled out as the input velocity changes. However, for multi-DOF mechanisms, the velocity ratios between any two input velocities become influential to the performance of the mechanisms. That is, different values of an input velocity ratio will result in different values of the EFR for the mechanism at the same configuration (posture). As a result, the force transmission performance of a multi-DOF mechanism will also be dependent on the velocity ratios between two input velocities. In general, the input velocity is a time-dependent function. Hence, the velocity ratio parameters should be taken as independent parameters as we perform the force transmissibility analysis for multi-DOF mechanisms.

Consider an N-DOF mechanism, whose input links are denoted by $l_{\text{in}(i)}$, $(i=1,2,...,N)$. The magnitude of the input velocity of $l_{\text{in}(i)}$ is denoted by $\omega_{\text{in}(i)}$ for a revolute joint type input and $\nu_{\text{in}(i)}$ for a prismatic joint type input. We then define the input velocity ratio (IVR, η_{jk}) between $\omega_{\text{in}(j)}$ and $\omega_{\text{in}(k)}$ as

$$\eta_{jk}=\frac{\omega_{\text{in}(j)}}{\omega_{\text{in}(k)}} \quad \text{for revolute input joints,}$$

$$\eta_{jk}=\frac{\nu_{\text{in}(j)}}{\nu_{\text{in}(k)}} \quad \text{for prismatic input joints,}$$

$$j=1,2,...,N,\ \ k=1,2,...,N,\ \ j\neq k. \tag{4}$$

For an N-DOF mechanism, there are $N(N-1)$ combinations of velocity ratios. For example, for the planar two-DOF, five-bar parallel manipulator shown in Figure 1(a), there are two sets of velocity ratios. That is,

$$\eta_{21}=\frac{\omega_{\text{in}(2)}}{\omega_{\text{in}(1)}}=\frac{\omega_5}{\omega_2},$$

$$\eta_{12}=\frac{\omega_{\text{in}(1)}}{\omega_{\text{in}(2)}}=\frac{\omega_2}{\omega_5}. \tag{5}$$

The EFR and FTI of a mechanism at a configuration will be dependent on the IVR.

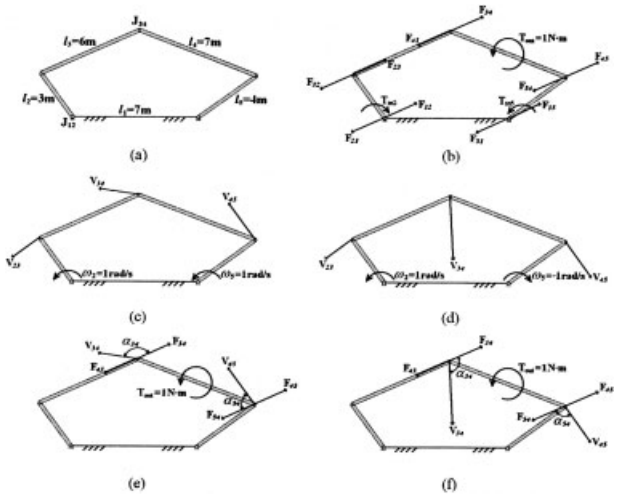

Figure 1. (a) A planar two-DOF, five-bar parallel manipulator. (b) The static force analysis. (c) The velocity analysis with $\omega_2=1$ rad/s and $\omega_5=1$ rad/s. (d) The velocity analysis with $\omega_2=1$ rad/s and $\omega_5=-1$ rad/s. (e) The combination of the result in (b) and (c). (f) The combination of the result in (b) and (d).

To demonstrate the influence of the velocity ratios, the planar two-DOF, five-bar parallel manipulator shown in Figure 1(a) is analyzed. Let the position of the fixed joint J_{12} be at the origin of the global coordinate system, and the position of the joint J_{34} be located at $(x=5,\ y=5)$ at a specific instant. First we perform the inverse displacement analysis to obtain the input displacement and the position of each link. Then we start evaluating the EFR and FTI of the mechanism by applying (1) and (2). The functional relationships between the EFR versus the IVR, and the FTI versus the IVR, are investigated by changing the values of the independent parameters (η_{12} and η_{21}). In each case the value of the denominator of the independent parameter is always kept at a constant input velocity of 1(rad/s). Figure 2 shows the plots of the EFR and FTI of the output link (l_4) as a function of the IVR at the specific configuration. We may conclude from the analysis that the EFR and FTI of a multi-DOF mechanism at a specific configuration are a function (instead of a fixed value) of the IVR. In general, it is desirable to represent the performance of a mechanism at a specific configuration by a definite value. In what follows, we shall introduce a new force transmission index to describe the force transmissibility performance of a multi-DOF mechanism. The index will yield a definite value for a specific configuration for multi-DOF mechanisms.

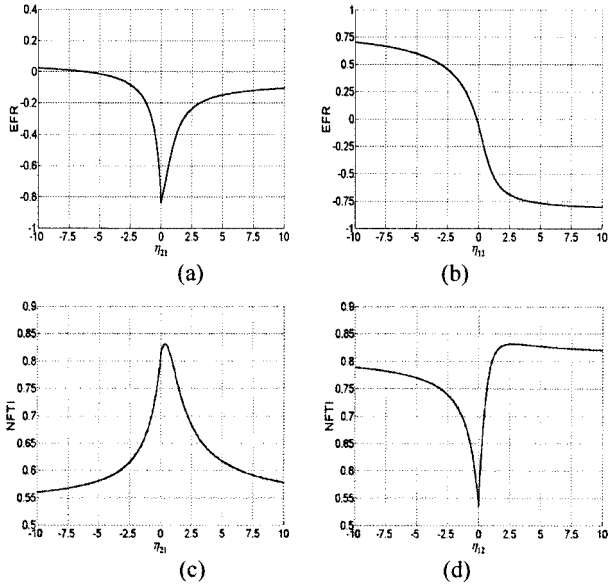

Figure 2. The performance of the mechanism in Figure 1. (a) EFR vs η_{21}. (b) EFR vs η_{12}. (c) FTI vs η_{21}. (d) FTI vs η_{12}.

3.2. Mean Force Transmission Index

Consider an N-DOF parallel manipulator with N limbs, assuming that there is one actuator mounted in each limb, hence the parallel manipulator has N independent input-related paths. According to (2), the individual force transmissibility of the pth input-related path (limb) can be described by

$$\tau^{(p)} = |R_i^{(p)} \cdot (MA)^{(p)}|, \quad p = 1,..,N, \tag{6}$$

where the superscript p denotes the index of the input-related path, and the subscript i denotes the index of the output link.

Since the moving platform (output link) is supported by the N limbs, it is reasonable to think that each individual limb will share its contribution in the force transmissibility of the mechanism. In other words, the force transmissibility of the parallel manipulator can be derived by summing up the individual force transmissibility of each limb. Thus the force transmissibility of the mechanism (at a specific posture) can be obtained by

$$\tau = \sum_{p=1}^{N} \tau^{(p)}. \tag{7}$$

The $NFTI(\tau_n)$ of the mechanism is obtained by substituting τ into (3), that is,

$$\tau_n = 1 - e^{-\lambda \tau}. \tag{8}$$

The above equation, however, does not yield a definite value, because τ or $\tau^{(p)}$ is a function of the IVR as we have known from the above paragraph. To represent the normalized force transmissibility of the parallel manipulator by a single definite value, we suggest to use the mean value ($\bar{\tau}_n$) of $NFTI$'s function over the whole range of the IVR, that is,

$$\bar{\tau}_n = \frac{\overbrace{\int_{-\infty}^{\infty}\int_{-\infty}^{\infty}\cdots\int_{-\infty}^{\infty}(\tau_n)d\,\eta_{12}d\,\eta_{13}\cdots d\,\eta_{1N}d\,\eta_{21}d\,\eta_{23}\cdots d\,\eta_{N(N-1)}}^{N(N-1)\text{multiples integrations}}}{\int_{-\infty}^{\infty}\int_{-\infty}^{\infty}\cdots\int_{-\infty}^{\infty}d\,\eta_{12}d\,\eta_{13}\cdots d\,\eta_{1N}d\,\eta_{21}d\,\eta_{23}\cdots d\,\eta_{N(N-1)}} \tag{9}$$

where $\eta_{ij}\,(i \neq j)$ denotes the IVR, which is defined in (4).

In computing τ_n, it is required to specify the velocity of all input links. However, the independent parameter η_{ij} depends on the velocity of two input links. Thus we need to specify the velocity of an input link to be a constant during the computation process. In practice, the integration in (9) is carried out by

$$\bar{\tau}_n = \frac{1}{N}\sum_{k=1}^{N} \frac{\overbrace{\int_{-\rho}^{\rho}\int_{-\rho}^{\rho}\cdots\int_{-\rho}^{\rho}(\tau_{n(k)})d\,\eta_{1k}\cdots d\,\eta_{jk}\cdots d\,\eta_{Nk}}^{(N-1)\text{multiples integrations}}}{(2\rho)^{N-1}} \tag{10}$$

where $\tau_{n(k)}$ denotes the normalized force

transmissibility as the velocity of the kth input link is set to be 1 rad/s, and the first subscript of η_{jk} ranges from 1 to N, but $j \neq k$.

To implement the numerical integration, the lower and upper bounds of the integration in (10) are taken as definite values. In this paper we set ρ to be 10 based on the following consideration. The functional plots in Figure 2 show that the function of the EFR or FTI will asymptotically approach to a fixed value as the IVR diverges. Hence it is appropriate to select a cutoff value as the lower and upper bounds of the IVR. Figure 2 shows that the EFR and FTI have saturated as the IVR attains ± 10.

The index $\bar{\tau}_n$ defined by (10) is called the *mean force transmission index* ($MFTI$) of an N-DOF parallel manipulator. The index, ranging between zero and one, is used to represent the force transmissibility of an N-DOF parallel manipulator at a specific configuration. For a specific configuration of a parallel manipulator, the larger the index, the better the force transmissibility performance of the mechanism.

It follows that the $MFTI$ of the two-DOF, five-bar parallel manipulator shown in Figure 1(a) can be written as

$$\bar{\tau}_n = \frac{\int_{-\rho}^{\rho}(\tau_{n1})d\,\eta_{21}/2\rho + \int_{-\rho}^{\rho}(\tau_{n2})d\,\eta_{12}/2\rho}{2}, \quad (11)$$

and the $MFTI$ of the three-DOF, eight-bar 3-RRR parallel manipulator shown in Figure 4 can be written as

$$\bar{\tau}_n = \frac{\int_{-\rho}^{\rho}\int_{-\rho}^{\rho}(\tau_{n1})d\,\eta_{21}d\,\eta_{31}/(2\rho)^2 + \int_{-\rho}^{\rho}\int_{-\rho}^{\rho}(\tau_{n2})d\,\eta_{12}d\,\eta_{32}/(2\rho)^2 + \int_{-\rho}^{\rho}\int_{-\rho}^{\rho}(\tau_{n3})d\,\eta_{13}d\,\eta_{23}/(2\rho)^2}{3}. \quad (12)$$

Below we summarize the force transmissibility analysis procedure in the following steps.

S1. Perform the inverse displacement analysis to obtain the configurations of the multi-DOF parallel manipulator.

S2. Perform the static force analysis to obtain the input-related joint forces of the moving platform.

S3. Apply (4) to find all the IVRs.

S4. Apply (6)–(8) to compute the $NFTI$ ($\tau_{n(k)}$) of the mechanism given a constant velocity ($\omega_{\text{in}(k)} = 1$ rad/s) of input link $l_{\text{in}(k)}$.

S5. Apply (10) to yield the $MFTI$ for the parallel manipulator at the specific configuration.

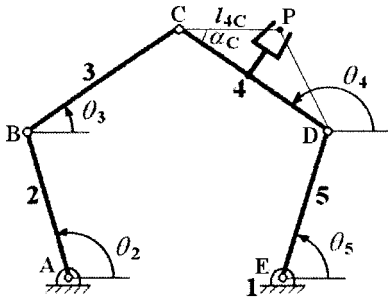

Figure 3. A planar two-DOF, five-bar parallel manipulator.

4. EXAMPLES

We shall illustrate the force transmissibility analysis procedure using the $MFTI$ method by two examples. The result will be compared with that of two other methods, namely, the Jacobian matrix method and the joint force index method.

4.1. Planar Two-DOF, Five-Bar Parallel Manipulator (An Asymmetric Manipulator Case)

For the planar two-DOF, five-bar parallel manipulator shown in Figure 3, let links 2 and 5 be the input and link 4 the output link. The link lengths are given as follows: $l_1 = 7$ m, $l_2 = 3$ m, $l_3 = 6$ m, $l_4 = 7$ m, and $l_5 = 4$ m. By differentiating the loop closure equation with respect to time, the relationship between the input angular velocity vector and the end-effector's velocity vector can be derived as follows:

$$\begin{bmatrix} \dot{x}_P \\ \dot{y}_P \end{bmatrix} = \begin{bmatrix} a_{11} & a_{12} \\ a_{21} & a_{22} \end{bmatrix} \begin{bmatrix} \dot{\theta}_2 \\ \dot{\theta}_5 \end{bmatrix}, \quad (13a)$$

where

$$a_{11}=-l_2\sin\theta_2-l_3h_1\sin\theta_3-l_{4C}h_2\sin(\theta_4+\alpha_C-\pi),$$

$$a_{12}=-l_3h_3\sin\theta_3-l_{4C}h_4\sin(\theta_4+\alpha_C-\pi),$$

$$a_{21}=l_2\cos\theta_2+l_3h_1\cos\theta_3+l_{4C}h_2\cos(\theta_4+\alpha_C-\pi), \tag{13b}$$

$$a_{22}=l_3h_3\cos\theta_3+l_{4C}h_4\cos(\theta_4+\alpha_C-\pi),$$

and where $l_{4C}=\overline{CP}$, $\alpha_C=\angle PCD$ are depicted in Figure 3. The parameters h_1, h_2, h_3, and h_4 are given as follows:

$$h_1=\frac{l_2\sin(\theta_4-\theta_2)}{l_3\sin(\theta_3-\theta_4)},$$

$$h_2=\frac{l_2\sin(\theta_3-\theta_2)}{l_4\sin(\theta_3-\theta_4)},$$

$$h_3=\frac{l_5\sin(\theta_5-\theta_4)}{l_3\sin(\theta_3-\theta_4)}, \tag{13c}$$

$$h_4=\frac{l_5\sin(\theta_5-\theta_3)}{l_4\sin(\theta_3-\theta_4)}.$$

Eq. (13a) can be rearranged in the following form,

$$J_q\begin{bmatrix}\dot\theta_2\\ \dot\theta_5\end{bmatrix}=J_x\begin{bmatrix}\dot x_P\\ \dot y_P\end{bmatrix}, \tag{14a}$$

where

$$J_q=l_3l_4\sin(\theta_3-\theta_4)\begin{bmatrix}a_{11}&a_{12}\\ a_{21}&a_{22}\end{bmatrix} \tag{14b}$$

is the inverse Jacobian matrix, and

$$J_x=\begin{bmatrix}l_3l_4\sin(\theta_3-\theta_4)&0\\ 0&l_3l_4\sin(\theta_3-\theta_4)\end{bmatrix} \tag{14c}$$

is the forward Jacobian matrix.

The determinant of the forward Jacobian matrix can be expressed as

$$\mathrm{Det}(J_x)=l_3^2l_4^2\sin^2(\theta_3-\theta_4). \tag{15}$$

In (15), we may observe that as links 3 and 4 become collinear, the five-bar parallel manipulator is located at the direct kinematic singularity, corresponding to the locking position of the manipulator. The position, also referred to as the singular position, is conventionally regarded as the worst configuration in motion transmissibility.

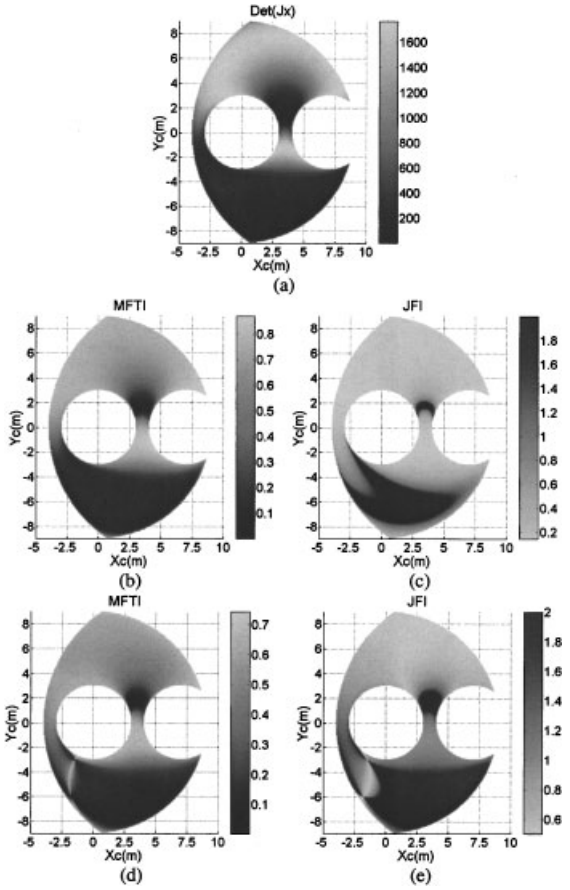

Figure 4. The result for a planar two-DOF, five-bar parallel manipulator. (a) The determinant of the forward Jacobian matrix. (b) The *MFTI* map with a unit moment loading. (c) The *JFI* map with a unit moment loading. (d) The *MFTI* map with a unit force loading. (e) The *JFI* map with a unit force loading.

In this example two kinds of loading are exerted on the output link individually. That is, a pure moment with the magnitude of $T_{\mathrm{out}}=1(N-m)$, and a pure force, $\mathbf{F}_{\mathrm{out}}=(-1/\sqrt{2},-1/\sqrt{2})N$, exerted on the centroid of link 4. Then we apply (11) to evaluate the *MFTI* of the five-bar parallel manipulator within its reachable workspace. The workspace of the two-DOF parallel manipulator is formed by the locating all the positions that joint J_{34} (point *C*) can reach. We have derived the maps of the *MFTI*, the determinant of the forward Jacobian matrix and the *JFI*. Figure 4 shows the result for one of the four possible configurations. Figure 4(a) shows the map of the determinant

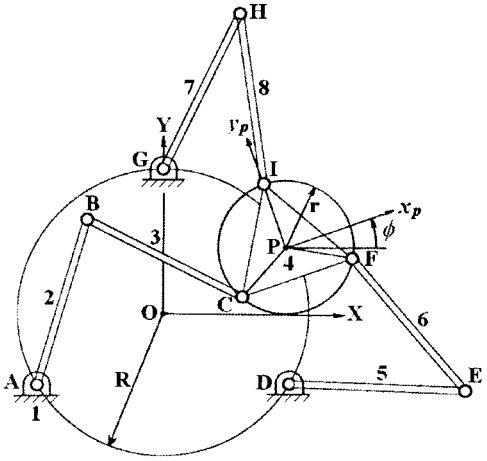

Figure 5. A planar three-DOF, eight-bar parallel manipulator.

of the forward Jacobian matrix. Figures 4(b) and 4(c) show the maps of $MFTI$ and JFI for the case of a pure moment loading. Figures 4(d) and 4(e) show the maps of $MFTI$ and JFI for the case of a pure force loading.

4.2. Planar Three-DOF, Eight-Bar Parallel Manipulator (A Symmetric Manipulator Case)

For the planar three-DOF, eight-bar parallel manipulator shown in Figure 5, the inverse displacement analysis is performed to determine the input joint displacements. In the example, the input angular displacements, denoted by θ_2, θ_5, and θ_7, are measured counterclockwise from the positive X-axis to the longitudinal axes of the input links. The position of a reference point P at the platform (link 4) is described by (X_P, Y_P) with respect to the global coordinate system O-XY, while the orientation of the platform is described by the angle ϕ measured counterclockwise from the positive X-axis to the positive x_p-axis of the local coordinate system P-$x_p y_p$ attached to the platform. In Figure 5, the fixed pivots J_{12}, J_{15}, and J_{17} (points A, D, and G) at the base link form an equilateral triangle, where $\angle AOD = \angle AOG = \angle DOG = 120°$. The moving pivots J_{34}, J_{64}, and J_{84} (points C, F, and I) on the moving platform also form an equilateral triangle, where $\angle CPF = \angle CPI = \angle FPI = 120°$. The three fixed pivots on the base link lie on a circle whose center is the origin O and radius is R, and the three moving pivots on the platform lie on a circle whose center is the local origin P and radius is r. The geometric lengths are given as follows: $R = 3$ m, $r = 2\sqrt{3}/3$ m, $l_2 = l_5 = l_7 = 2$ m, and $l_3 = l_6 = l_8 = 3$ m. By using the geometric analytical method, given the position and orientation (X_P, Y_P, ϕ), the input joint angles (θ_2, θ_5, and θ_7) can be obtained. Totally, there are eight configurations existing for a given position and orientation of the moving platform. The constant orientation workspace of the platform can be determined by fixing the angle ϕ at a given value, and then verifying the existence of the solution of the inverse displacement analysis, with a valid position of the point P in the workspace.

Again by differentiating the loop closure equation with respect to time, the relationship between the input velocity vector and the velocity vector of the platform can be derived as follows:

$$J_q \begin{bmatrix} \omega_2 \\ \omega_5 \\ \omega_7 \end{bmatrix} = J_x \begin{bmatrix} \nu_{Px} \\ \nu_{Py} \\ \phi \end{bmatrix}, \tag{16a}$$

where

$$J_q = \begin{bmatrix} l_{2x} l_{3y} - l_{2y} l_{3x} & 0 & 0 \\ 0 & l_{5x} l_{6y} - l_{5y} l_{6x} & 0 \\ 0 & 0 & l_{7x} l_{8y} - l_{7y} l_{8x} \end{bmatrix} \tag{16b}$$

and

$$J_x = \begin{bmatrix} l_{3x} & l_{3y} & l_{PCx} l_{3y} - l_{PCy} l_{3x} \\ l_{6x} & l_{6y} & l_{PFx} l_{6y} - l_{PFy} l_{6x} \\ l_{8x} & l_{8y} & l_{PIx} l_{8y} - l_{PIy} l_{8x} \end{bmatrix}. \tag{16c}$$

The expression for the determinant of the forward Jacobian matrix J_x is expressed as

$$\begin{aligned} \mathrm{Det}(J_x) = l_3 l_6 l_8 [& l_{PC} \sin(\theta_8 - \theta_6) \sin(\theta_3 - \phi - \phi_{PC}) \\ & + l_{PF} \sin(\theta_3 - \theta_8) \sin(\theta_6 - \phi - \phi_{PF}) \\ & + l_{PI} \sin(\theta_6 - \theta_3) \sin(\theta_8 - \phi - \phi_{PI})]. \end{aligned} \tag{17}$$

The same loadings (a pure moment and a pure force) as in the above example are exerted on the platform (link 4) individually. Then we apply (12) to evaluate the $MFTI$ of the eight-bar parallel manipulator within its workspace. The constant-orientation workspace is constructed by locating all reachable positions of the point P with the orientation angle ϕ=0°. Figures 6 show the analysis result for one of the eight possible configurations. Among them, Figure 6(a) shows the map of the determinant of the forward

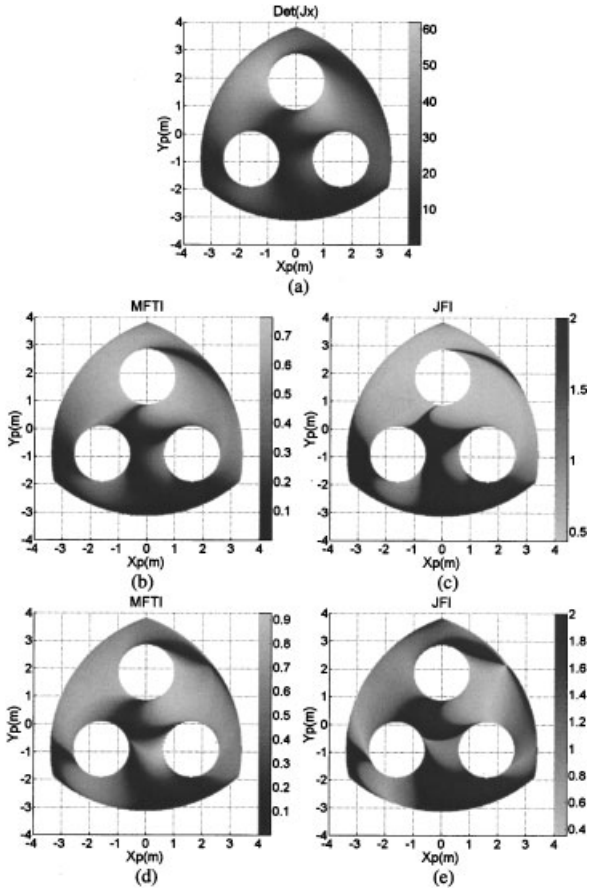

Figure 6. The results for a planar three-DOF, eight-bar parallel manipulator. (a) The determinant of the forward Jacobian matrix. (b) The *MFTI* map with a unit moment loading. (c) The *JFI* map with a unit moment loading. (d) The *MFTI* map with a unit force loading. (e) The *JFI* map with a unit force loading.

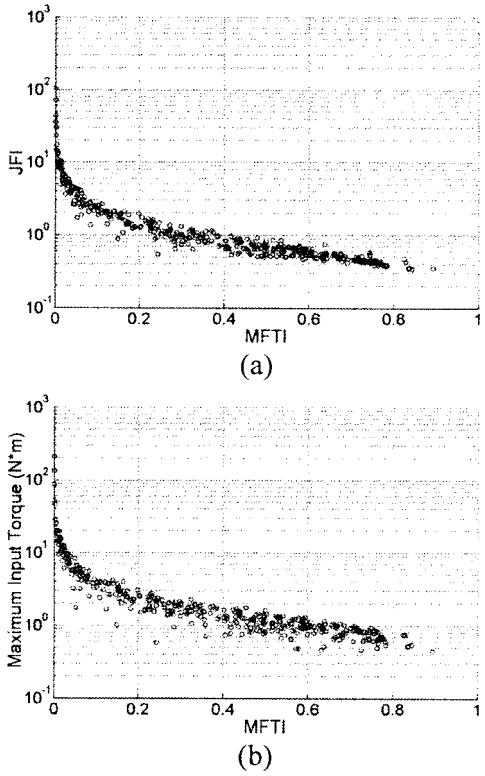

Figure 7. (a) The relationship between *JFI* and *MFTI* of a three-DOF parallel manipulator. (b) The relationship between maximum input torque and *MFTI* of a three-DOF parallel manipulator.

Jacobian matrix, Figures 6(b) and 6(c) show the maps of *MFTI* and *JFI* for the case of the pure moment loading, and Figures 6(d) and 6(e) show the maps of *MFTI* and *JFI* for the case of the pure force loading.

Observing Figures 4 and 6, we find that the *MFTI* and *JFI* can describe the singular curves (darkest areas) within the workspace as the determinant of the forward Jacobian matrix does. In fact, the locations of the singular curves described by the three methods are in accordance. On the other hand, the locations of the best-performance areas (lightest areas) described by the three methods are different. As we have known, the determinant of the forward Jacobian matrix is configuration dependent only and will not reflect the influence of different types of the loading. The map shown in Figures 5(a) and 6(a) can only provide the information about the "distance" away from the singularities but not force transmissibility performance. Considering the behavior corresponding to different types of loadings, both the *MFTI* and *JFI* seem to be proper force performance indices, as we compare between Figures 4(b) and 4(d), and Figures 4(c) and 4(e).

The *JFI*,[32] defined as the ratio of the maximum joint force magnitude among all the joints of a mechanism to the magnitude of the loading, is considered as a significant representation of the static force characteristics of mechanisms. Usually, as the *JFI* becomes smaller, the force transmission performance tends to be better. In what follows, we shall investigate the relationship between the *JFI* and the *MFTI*, and the maximum input torque and the *MFTI*. To find the functional relationship, the *MFTI*, *JFI*, and maximum input torque are evaluated at all sampled positions uniformly distributed in the overall workspace of the three-DOF, eight-bar parallel manipulator. The sampled positions (including orientations) of the platform are stated as follows:

$$S=\{(X_p, Y_p, \phi) | -4 \leqslant X_p \leqslant 4,\ \Delta X_p = 0.5;\quad -4 \leqslant Y_p \leqslant 4,\ \Delta Y_p = 0.5;\quad 0° \leqslant \phi \leqslant 360°,\ \Delta\phi = 45°\}. \tag{18}$$

Finally, the functional relationship of the *JFI* versus *MFTI*, and the maximum input torques versus *MFTI* are shown in Figures 7(a) and 7(b), respectively. The plots show that the *JFI* and the maximum input torque are approximately inversely proportional to the *MFTI*. The above evaluation is based on the case of a unit moment loading. A similar result can be obtained for the case of a unit force loading. The result suggests that, as a general trend, when the maximum joint force or the maximum input torque decreases, the force transmission performance becomes better (as the value of the *MFTI* increases). It indicates, generally, as the *MFTI* increases the mechanism requires less torque/force to resist the loading. On the other hand, as the mechanism's configuration is near a singularity, the *MFTI* tends to be zero, while the maximum joint force and the maximum input torque diverge. Consequently, the *MFTI* is proved to be a proper and useful index for describing the force transmissibility performance of symmetric parallel manipulators. The relationship, however, does not exist in the result for asymmetric parallel manipulators. Note that the above inverse-proportionality relationship is not perfectly deterministic. As we observe from Figure 7(b), a configuration with a larger value of the *MFTI* may have a larger maximum input torque than another configuration with a smaller *MFTI* value. That is, the *JFI* or the maximum input torque alone is not good enough to represent the force transmissibility performance of a mechanism.

5. DESIGN OPTIMIZATION

The proposed *MFTI* is the quantitative measure of the force transmissibility performance of parallel manipulators under a specific configuration. It is desirable to perform the design optimization by using the global *MFTI* as an objective function for a parallel manipulator. We define the global force transmission index (*GFTI*) as

$$\tau_g = \frac{\int_\Omega \bar{\tau}_n \, d\Omega}{\int_\Omega d\Omega}, \tag{19}$$

where Ω denotes the desired fine-performance workspace of a parallel manipulator, which can be a full workspace, a constant-orientation workspace, or a partial area of the said workspace. $\bar{\tau}_n$ denotes the *MFTI* of a parallel manipulator for a specific configuration, as defined in (10).

Thus the *GFTI* (τ_g) represents the mean value of the *MFTI* in the desired fine-performance workspace of a parallel manipulator. In what follows, we shall optimize the link lengths of the symmetric planar three-DOF, parallel manipulator mentioned in the above section. Assume that the three input links are equal in length, and the three coupler links are also equal in length (refer to Figure 4), that is, $l_{\text{in}} = l_2 = l_5 = l_7$, and $l_c = l_3 = l_6 = l_8$. The other design parameters are the radius of the lower platform (R), and the radius of the upper platform (r). Taking R as the base length, the nondimensional design parameters vector can be simplified as

$$\mathbf{x} = \left[\frac{r}{R}, \frac{l_{\text{in}}}{R}, \frac{l_c}{R}\right]^T. \tag{20}$$

The desired fine-performance workspace Ω is given as follows:

$$\Omega = \{(X_p, Y_p, \phi) | X_p^2 + Y_p^2 \leqslant (0.25R)^2 \wedge \phi = 0°\}. \tag{21}$$

Hence the optimal design problem is stated as follows:

Maximize

$$f(\mathbf{x}) = \tau_g \tag{22}$$

Subjected to

$$0.3 \leqslant \frac{r}{R} \leqslant 1.2, \tag{23a}$$

$$0.2 \leqslant \frac{l_{\text{in}}}{R} \leqslant 2.0, \tag{23b}$$

$$0.2 \leqslant \frac{l_c}{R} \leqslant 2.0, \tag{23c}$$

$$|\text{Det}(J_x)| > 0 \quad \text{for } (X_p, Y_p, \phi) \in \Omega. \tag{23d}$$

The last constraint in (23d) is to guarantee that no singularity exists in the desired workspace Ω.

The nonlinear multi-constraint optimization problem can't be solved analytically. Hence we use the sequential quadratic programming (SQP) method to search the optimal solution. The direction search

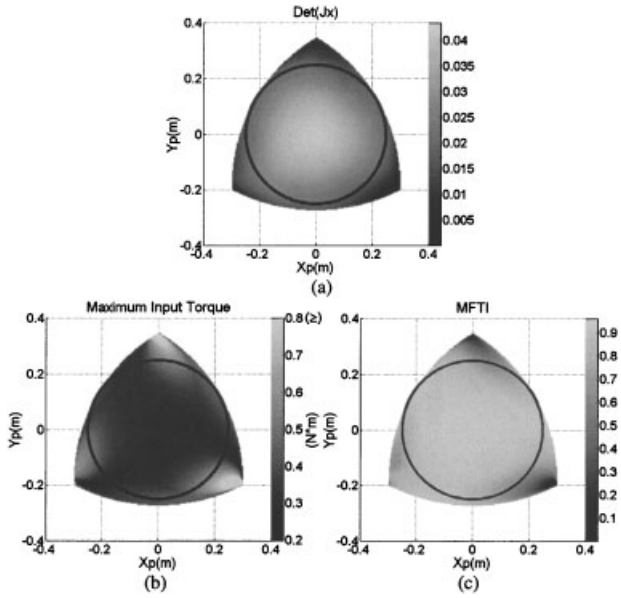

Figure 8. The performance of the planar three-DOF, parallel manipulator with optimal link lengths. (a) The determinant of the forward Jacobian matrix. (b) The maximum input torque (c) The *MFTI* map.

algorithm we used is the quasi-Newton method, and the Hessian matrix is estimated by the Broyden-Fletcher-Goldfarb-Shanno (BFGS) formula. The convergence tolerances are given as follows: ε(design variables)=5×10^{-4}, ε(constraint violation)=5×10^{-4}, and ε(objective function)=5×10^{-8}. We utilize the MATLAB Optimization Toolbox[36] to undertake the computation.

Given the initial guess values of the design parameters as $\mathbf{x_0}=[0.625,0.4,0.4]^T$, the optimal design parameters obtained are

$$\left(\frac{r}{R}\right)^* = 0.6277,$$

$$\left(\frac{l_{\text{in}}}{R}\right)^* = 0.2986,$$

$$\left(\frac{l_c}{R}\right)^* = 0.3237,$$

with the maximum global force transmission index $\tau_g^* = 0.902\,420\,5$.

To verify the performance of the parallel manipulator with the optimal link lengths, we proceed to evaluate the determinant of the forward Jacobian matrix, the maximum input torque, and the *MFTI*, given $R=1$(m), with a unit moment loading. Figures 8(a)–8(c) show the maps of the determinant of the forward Jacobian matrix, the maximum input torque, and the *MFTI*, respectively. The area inside the circle in each map represents the desired fine-performance workspace we specified in the beginning of the optimization process. The result shows that there is no singularity inside the desired workspace Ω, the maximum input torque in most area of Ω is less than 0.4(N-m) (40% of the loading), and the *MFTI* in most area of Ω is greater than 0.8. The result confirms our expectation of fine force transmissibility performance.

6. CONCLUSIONS

In this paper we have proposed a new force transmission index called the *MFTI* and establish the force transmissibility analysis procedure for parallel manipulators. The *MFTI* is derived from the definition of the *FTI* introduced by the authors previously. It is found that the *FTI* is a function of the *IVR* (in stead of a definite value) for multi-DOF mechanisms at a specific posture. To represent the force transmissibility of a multi-DOF mechanism at a specific posture by a definite value, the *MFTI* is defined by the mean value of the normalized *FTI*'s function over the whole range of the input velocity ratio. Performance analysis of two planar parallel manipulators is illustrated using the *MFTI* method, the determinant of the forward Jacobian matrix and *JFI* methods. The result shows that the *MFTI* can describe the force transmission performance of parallel manipulators more accurately. In addition, especially for the symmetric parallel manipulators, an approximate inverse-proportionality relationship exists between the *JFI* and *MFTI*, and between the maximum input torque/force and *MFTI*. We conclude that the *MFTI* is a significant force performance index for multi-DOF parallel manipulators. Finally, the design optimization problem is studied by taking the global force transmission index as the objective function. The performance analysis result of the optimal design confirms our initial goal.

REFERENCES

1. C.M. Gosselin and J. Angeles, Singularity analysis of closed-loop kinematic chains, IEEE Trans Robot Automat 6 (1990), 281–290.
2. D. Zlatanov, R.G. Fenton, and B. Benhabib, Singularity analysis of mechanisms and robots via a motion-space

model of the instantaneous kinematics, Proc IEEE Int Conf Robotics Automat, 1994, pp. 980–991.
3. J. Sefrioui and C.M. Gosselin, Singularity analysis and representation of planar parallel manipulators, Robot Autonom Syst 10 (1992), 209–224.
4. J. Sefrioui and C.M. Gosselin, On the quadratic nature of the singularity curves of planar three-degree-of-freedom parallel manipulators, Mech Mach Theory 30 (1995), 533–551.
5. M.H.R. Daniali, P.J. Zsombor-Murray, and J. Angeles, Singularity analysis of planar parallel manipulators, Mech Mach Theory 30 (1995), 665–678.
6. B.M. St-Onge and C.M. Gosselin, Singularity analysis and representation of the general Gough-Stewart platform, Int J Robot Res 19 (2000), 271–288.
7. P. Choudhury and A. Ghosal, Singularity and controllability analysis of parallel manipulators and closed-loop mechanisms, Mech Mach Theory 35 (2000), 1455–1479.
8. M. Gallant and R. Boudreau, The synthesis of planar parallel manipulators with prismatic joints for an optimal, singularity-free workspace, J Robot Syst 19 (2002), 13–24.
9. S.A. Joshi and L.W. Tsai, Jacobian analysis of limited-DOF parallel manipulators, Trans ASME J Mech Des 124 (2002), 254–258.
10. F.C. Park and J.W. Kim, Manipulability of closed kinematic chains, Trans ASME J Mech Des 120 (1998), 542–548.
11. J.T. Wen and L.S. Wilfinger, Kinematic manipulability of general constrained rigid multibody systems, IEEE Trans Robot Automat 15 (1999), 558–567.
12. K.-S. Hong and J.-G. Kim, Manipulability analysis of a parallel machine tool: Application to optimal link length design, J Robot Syst 17 (2000), 403–415.
13. V. Kumar, Characterization of workspaces of parallel manipulators, Trans ASME J Mech Des 114 (1992), 368–375.
14. G.R. Pennock and D.J. Kassner, Workspace of a general geometry planar three-degree-of-freedom platform-type manipulator, Trans ASME J Mech Des 115 (1993), 269–276.
15. J.P. Merlet, Determination of the orientation workspace of parallel manipulators, J Intell Robotic Syst: Theory Appl 13 (1995), 143–160.
16. C.M. Gosselin and M. Jean, Determination of the workspace of planar parallel manipulators with joint limits, Robot Autonom Syst 17 (1996), 129–138.
17. J.P. Merlet, Designing a parallel manipulator for a specific workspace, Int J Robot Res 16 (1997), 545–556.
18. L.-C.T. Wang and J.-H. Hsieh, Extreme reaches and reachable workspace analysis of general parallel robotic manipulators, J Robot Syst 15 (1998), 145–159.
19. J.P. Merlet, C.M. Gosselin, and N. Mouly, Workspaces of planar parallel manipulators, Mech Mach Theory 33 (1998), 7–20.
20. J.P. Merlet, Determination of 6D workspaces of Gough-type parallel manipulator and comparison between different geometries, Int J Robot Res 18 (1999), 902–916.
21. J.A. Carretero, M.A. Nahon, and R.P. Podhorodeski, Workspace analysis and optimization of a novel 3-DOF parallel manipulator, Int J Robot Automat 15 (2000), 178–188.
22. C. Gosselin and J. Angeles, A global performance index for the kinematic optimization of robotic manipulators, Trans ASME J Mech Des 113 (1991), 220–226.
23. X.-J. Liu, Z.-L. Jin, and F. Gao, Optimum design of 3-DOF spherical parallel manipulators with respect to the conditioning and stiffness indices, Mech Mach Theory 35 (2000), 1257–1267.
24. L.W. Tsai and S. Joshi, Comparison study of architectures of four 3 degree-of-freedom translational parallel manipulators, Proc IEEE Int Conf Robotics Automat, Seoul, 2001, pp. 1283–1288.
25. F. Tahmasebi and L.W. Tsai, On the stiffness of a novel six-degree-of-freedom parallel minimanipulator, J Robot Syst 12 (1995), 845–856.
26. B.S. El-Khasawneh and P.M. Ferreira, Computation of stiffness and stiffness bounds for parallel link manipulators, Int J Mach Tools Manuf 39 (1999), 321–342.
27. M. Ceccarelli and G. Carbone, A stiffness analysis for CaPaMan (Cassino Parallel Manipulator), Mech Mach Theory 37 (2002), 427–439.
28. J. Denavit, R.S. Hartenberg, R. Razi, and J.J. Uicker, Jr., Velocity, acceleration, and static-force analysis of spatial linkages, Trans ASME J Appl Mech 32 (1965), 903–910.
29. F. Wu and H.M. Lankarani, A new parameter for transmission quality and output sensitivity analysis of mechanisms, Proc ASME Mech Conf, 1992, pp. 103–109.
30. M.J. Tsai and H.W. Lee, Generalized evaluation for the transmission performance of mechanisms, Mech Mach Theory 29 (1994), 607–618.
31. Y. Takeda and H. Funabashi, Motion transmissibility of in-parallel actuated manipulators, JSME Int J Ser C 38 (1995), 749–755.
32. J.E. Holte and T.R. Chase, A force transmission index for planar linkage mechanisms, Proc ASME Mech Conf, 1994, pp. 377–386.
33. C.C. Lin and W.T. Chang, The force transmissivity index of planar linkage mechanisms, Mech Mach Theory 37 (2002), 1465–1485.
34. C.C. Lin and W.T. Chang, Force transmissibility of planar multiloop linkages, J Mech Eng Sci, Proc Instn Mech Eng Part C (to be published).
35. W.T. Chang, On the force transmission performance of planar and spatial linkage mechanisms, master thesis, National Taiwan Ocean University, Taiwan, ROC, 2002.
36. MATLAB Optimization Toolbox User's Guide, Ver. 2.2, The Math Works, Inc., 2002.